Sustainable Energy & Fuels

Quaternized poly(arylene perfluoroalkylene)s (QPAFs) for alkaline fuel cells – a perspective

Journal:	*Sustainable Energy & Fuels*
Manuscript ID	SE-PER-02-2019-000106.R2
Article Type:	Perspective
Date Submitted by the Author:	08-May-2019
Complete List of Authors:	Miyake, Junpei; University of Yamanashi, Miyatake, Kenji; University of Yamanashi, Clean Energy Research Center

Sustainable Energy & Fuels

PERSPECTIVE

Quaternized poly(arylene perfluoroalkylene)s (QPAFs) for alkaline fuel cells – a perspective

Received 00th January 20xx,
Accepted 00th January 20xx

DOI: 10.1039/x0xx00000x

www.rsc.org/

Junpei Miyake[a] and Kenji Miyatake*[ab]

The recent progress of our research on quaternized poly(arylene perfluoroalkylene)s (QPAFs) as anion exchange membranes (AEMs) for alkaline fuel cell applications is reviewed. First, the effect of the perfluoroalkylene group in the polymer main chains on the AEM properties is discussed. We emphasize that the polymer main chains of QPAFs remain intact in the harsh alkaline environment, and QPAFs have desirable AEM properties, such as well-developed phase-separated morphology, good anion transport, mechanical robustness, and gas barrier properties. We then discuss the effect of the molecular structures of the quaternary ammonium groups on the alkaline stability of the QPAF membranes. A number of pendant ammonium head groups are much more alkaline-stable than the classical benzyltrimethylammonium groups. Comparison of our QPAFs with other state-of-the-art AEMs implies that well-designed aromatic AEMs are potentially applicable to alkaline fuel cells that use hydrogen or hydrazine as a fuel.

Introduction

Anion exchange membranes (AEMs) have attracted considerable attention in the last decade for a wide variety of applications, including redox flow batteries, electrodialyzers, water electrolyzers, and fuel cells (FCs).[1-10] Among these applications, anion exchange membrane fuel cells (AEMFCs) are known to have great advantages over their proton-type counterparts (PEMFCs). Particularly, high pH conditions of AEMFCs enable the use of abundant transition metals (e.g., Ni, Co, Fe) as electrocatalysts and enhance the oxygen reduction reaction kinetics while precious metal catalysts (e.g., Pt) are required under the strongly acidic conditions of typical PEMFCs.[11-13] However, critical issues of AEMFCs are sluggish kinetics of the hydrogen oxidation reaction in alkaline media, and rather low ion conductivity (in particular, at lower hydration levels, or at lower humidities in gas phases) and insufficient stability of AEMs, compared to PEMs.

In general, AEMs consist of polymer main chains functionalized with cationic groups. The most widely used cationic groups are quaternary ammonium groups due to their facile synthesis. Under high pH conditions, the ammonium-functionalized AEMs are known to experience chemical degradation via hydroxide ion attack. Some degradation mechanisms have been proposed, such as nucleophilic substitution (S_N2 reaction), Hofmann elimination (E2 elimination), Ei elimination, and rearrangements.[14–16] It is known that the degradation of AEMs occurs not only through a single mechanism but also through a combination of several mechanisms. Furthermore, the contribution of each mechanism depends on the structures of the polymer main chains and ammonium groups. Recently, it was also reported that alkaline media with lower water content significantly increased the degradation rate of ammonium groups, regardless of the mechanism of degradation.[17-19]

To improve the alkaline stability of AEMs, wide varieties of polymer main chains, ranging from aliphatic to aromatic structures as well as cation groups such as ammonium, phosphonium, sulfonium, and metal cations, have been investigated.[20-32] We have previously reported that quaternized poly(arylene ether)s had high hydroxide ion conductivity (e.g., 144 mS cm^{-1} at 80 °C in water), but their alkaline stability needed improvement.[33-37] It was reported that the quaternized poly(arylene ether)s had a high possibility to be degraded through the nucleophilic attack of hydroxide ions onto the ipso carbon in oxyphenylene groups.[38,39] Thus, non-use of aromatic ether linkages has become an essential molecular design feature for alkaline stable AEMs.

In 2015, we proposed a novel family of quaternized polymers, QPAFs [quaternized poly(arylene perfluoroalkylene)s], whose main chain consisted of aromatic rings and perfluoroalkylene groups and did not contain any heteroatom linkages such as aromatic ethers. Up to the present, QPAFs with wide varieties of molecular structures have been examined for better performing AEMs.[40-46] The objective of this Perspective is to provide a quick overview of the current state of our QPAFs for AEMFC applications. Because the polymer main chain is the most important part of the AEM, our discussion begins with the effect of the main chain structures of QPAFs on the AEM properties with the classical benzyltrimethylammonium groups. We then assess the effects of the pendant alkyl groups at the

[a] Clean Energy Research Center, University of Yamanashi, 4 Takeda, Kofu, Yamanashi 400-8510, Japan. Email: miyatake@yamanashi.ac.jp
[b] Fuel Cell Nanomaterials Center, University of Yamanashi, 4 Takeda, Kofu, Yamanashi 400-8510, Japan

benzylic nitrogen-centered cations, as well as the interstitial aliphatic groups between main chains and ammonium groups on the alkaline stability of QPAF membranes. Further, comparison of our QPAFs with other state-of-the-art AEMs is discussed in the last part of this Perspective.

Sustainable Energy & Fuels

PERSPECTIVE

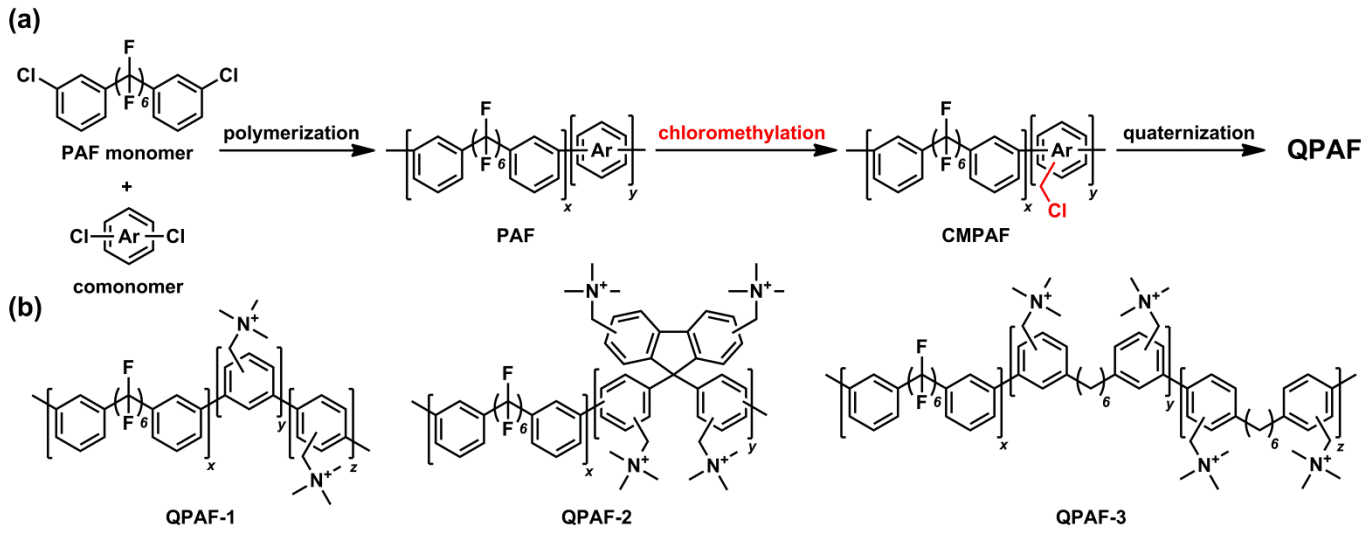

Scheme 1 (a) Synthesis and (b) molecular structure of QPAF-1[40], -2[41], and -3[43] via chloromethylation route.

QPAFs with benzyltrimethylammonium groups (QPAF-1[40], -2[41], and -3[43])

Synthesis of QPAF-1[40], -2[41], and -3[43]

Throughout this paper, bis(3-chlorophenyl)perfluorohexane (PAF monomer in Scheme 1a) is used as the common monomer, which consists of a linear perfluorohexane capped with two *m*-chlorophenylene groups. The PAF monomer was synthesized via Ullmann coupling of 1,6-diiodo-dodecafluorohexane and 1-chloro-3-iodobenzene using Cu powder as a catalyst in high yield (85%) and purity (> 99% by ^{1}H NMR). Scheme 1 illustrates the general synthetic method and molecular structure of QPAFs (QPAF-1, -2, and -3) via chloromethylation. The synthesis consists of Ni-mediated copolymerization, Friedel–Crafts chloromethylation, and quaternization, followed by ion exchange reactions.

The copolymerization of the PAF monomer and the corresponding comonomer was carried out using bis(1,5-cyclooctadiene) nickel(0) ($Ni(COD)_2$) as a mediator and 2,2'-bipyridine as a ligand. In the case of PAF-1 for example,[40] the use of the mixture (1,3- and 1,4-dichlorobenzenes) as the comonomer was important to provide PAF-1 (typically a white powder) with high molecular weight and high solubility in common organic solvents such as chloroform, TCE, and DMAc. By changing the feed comonomer ratio, wide varieties of compositions (i.e., *x*/*y*/*z* ratios) with supposed molecular structure were obtainable, which were well-characterized by ^{1}H and ^{19}F NMR spectra. PAF-2[41] and -3[43] were also successfully synthesized in a similar way.

The chloromethylation reaction of the PAF was conducted with chloromethyl methyl ether (CMME) using zinc chloride ($ZnCl_2$) as a Lewis acid catalyst and, in some cases, thionyl chloride ($SOCl_2$) as a promoter. The position and number of introduced chloromethyl groups depend on the steric and electronic environment of the aromatic moieties as well as the reaction conditions (i.e., concentration of the reactants, temperature, etc.). In the case of PAF-2, for example, the chloromethylation reaction proceeded preferentially at the less crowded and more electron-rich aromatic rings (i.e., fluorenyl groups), and then at the more crowded aromatic ring (i.e., phenylene groups in the main chain in the *y* part). In all cases (PAF-1, -2, and -3), within the reaction conditions we tested, the phenylene rings attached to the perfluoroalkyl chains (i.e., *x* part) remained intact due to the strong electron-withdrawing nature of the perfluoroalkyl groups. The degree of chloromethylation (DC, defined as the number of chloromethyl groups per phenylene group in the *y* and/or *z* parts) values ranged from 0.43 to 1 (DC = 1 means each phenylene group in the *y* and/or *z* parts was substituted with one chloromethyl group), which were calculated from the integral ratios of aromatic peaks to methylene peaks in ^{1}H NMR spectra. In most cases, the CMPAFs were soluble in common organic solvents (in some cases, better solubility than the parent PAFs), implying negligible or minor cross-linking reaction.

The quaternization (or Menschutkin) reaction took place with trimethylamine aqueous solution. In the case of CMPAF-1, the reaction was conducted in a homogeneous system, and the recovered QPAF-1 solid was cast from DMSO solution to obtain QPAF-1 membrane (in Cl^- form). In the case of CMPAF-2 and -3,

the reaction was conducted in a heterogeneous system, i.e., the pre-cast CMPAF membranes were soaked in trimethylamine aqueous solution to obtain QPAF-2 and- 3 membranes (in Cl^- forms). In general, the quaternization reaction was quantitative, and the ion exchange capacity (IEC) valued determined from ^1H NMR spectra and titration (Mohr method) were in good accordance, within acceptable error. Note that no detectable side reactions occurred at the perfluoroalkylene groups throughout the synthesis.

Since OH^- reacts with CO_2 in the atmosphere, we evaluated the properties mostly in Cl^- form, even though these properties might be affected by the counter-anion.[47] Transmission electron microscopic (TEM) observation was conducted with membranes in $PtCl_4^{2-}$ form to enhance the contrast. The OH^- conductivity was measured in degassed and deionized water (18 MΩ) to minimize the effect of CO_2. However, since the carbonation process of OH^- might not be avoidable completely, the reported OH^- conductivity herein might be lower than the true OH^- conductivity (i.e., CO_2-free, 100% OH^- anion).[48,49] More detailed measurement conditions can be found in our original papers.[40-46]

Properties of QPAF-1[40], -2[41], and -3[43]

Since detailed data and discussion have also been already published,[40-46] we provide herein a quick overview, focusing on some important characteristic data of these QPAF membranes. Morphology of the QPAF membranes was observed by TEM. Generally, ionomer membranes exhibit phase-separated morphology based on the hydrophilic-hydrophobic differences of their components. For QPAF membranes, high flexibility and hydrophobicity of the perfluoroalkylene groups in the main chain were expected to enhance the phase-separation. For example, in the case of QPAF-1 membrane (IEC = 1.26 meq g^{-1}), the hydrophilic domains were spherical (ca. 1.6 nm in diameter), and the hydrophobic domains were ca. 1.0 nm in diameter (Fig. 1a).[40] The random copolymer structure of QPAF-1 would be responsible for such small phase-separated morphology, which was similar to the well-known morphology of random copolymer-based proton conductive ionomer (Nafion) membrane (i.e., spherical hydrophilic domains of ca. 4 - 5 nm surrounded by hydrophobic domains of a similar size). (Note that several morphological models have been proposed for Nafion, depending on the hydration levels: Cluster-network model, cylindrical or layered model, rod-like elongated polymer aggregate model, locally flat ribbon-like model, etc.[50]) Besides, the molecular structure also seemed to affect the domain size to some extent. The hydrophilic and hydrophobic domains in QPAF-2 membrane (IEC = 1.1 meq g^{-1}) were of ca. 5 - 10 nm and ca. 5 - 10 nm diameter (data not shown),[41] respectively, which were larger than those of the above QPAF-1 membrane, probably due to bulkier structure of the fluorenyl groups as scaffold for the ammonium groups. QPAF-3 membranes with comparable IEC (1.4 meq g^{-1}) but different *m*- and *p*-phenylene compositions (i.e., *y*/*z* ratios) showed different morphology (data not shown).[43] QPAF-3 membrane with no *p*-phenylene (i.e., no *z* part) contained hydrophilic and hydrophobic domains of ca. 3.5 and 7.3 nm in diameter, larger than those of QPAF-1 membrane. QPAF-3 membrane with the highest *p*-phenylene content (i.e., no *y* part) exhibited more developed phase separation with interconnected hydrophilic domains. Its hydrophilic and hydrophobic domains were ca. 6.0 and 8.0 nm in diameter, suggesting that the more symmetrical structure of *p*-phenylene groups in comparison with *m*-phenylene groups in the hydrophilic moieties seemed to contribute to self-aggregation of the hydrophilic components, resulting in the well-developed interconnected ionic channels.

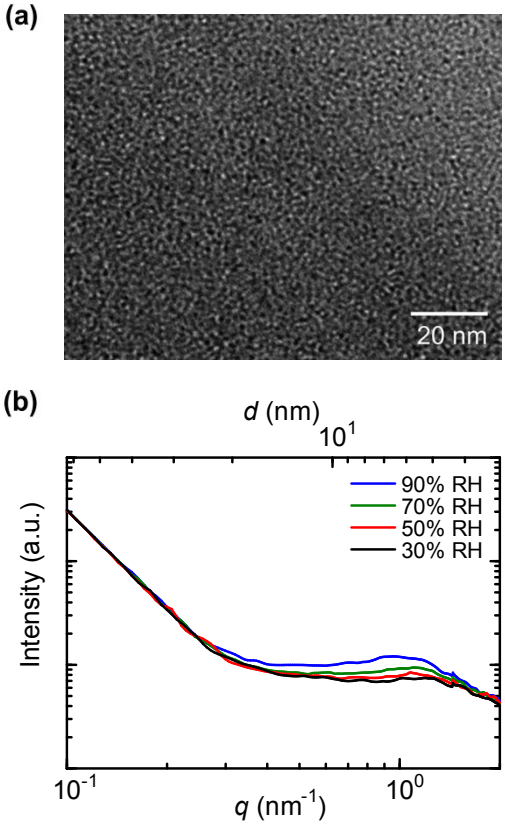

Fig. 1 (a) TEM image[40] (in $PtCl_4^{2-}$ forms) and (b) SAXS profiles[46] (in Cl^- forms) of QPAF-1 membrane (IEC = 1.26 meq g^{-1}) as a function of the scattering vector (*q*) value at 40 °C.

Since the above TEM images only provide morphological information of the membranes with no (or very low) hydration level, further investigation needs to be conducted under practical conditions (e.g., higher temperature with significant humidity). The morphological change with humidity was investigated by small-angle X-ray scattering (SAXS) at 40 °C and various humidities. In the SAXS profiles of the QPAF-1 membrane (IEC = 1.26 meq g^{-1} in Cl^- form),[46] a broad peak was observed at ca. 1 nm^{-1} of the scattering vector (*q*) or 6 nm of the *d* spacing at 30% RH (relative humidity), which developed as the humidity increased (Fig. 1b). The *d* value was ca. 7 nm at 90% RH. Similarly, QPAF-2 membrane (IEC = 1.0 meq g^{-1} in Cl^- form) showed a peak at ca. *d* = 8 nm at 30% RH, which developed more with increasing humidity (ca. *d* = 9 nm at 90%

RH, data not shown).[41] It is assumed that the observed *d* spacings in the SAXS profiles are related to the periodic structure of the hydrophilic domains.

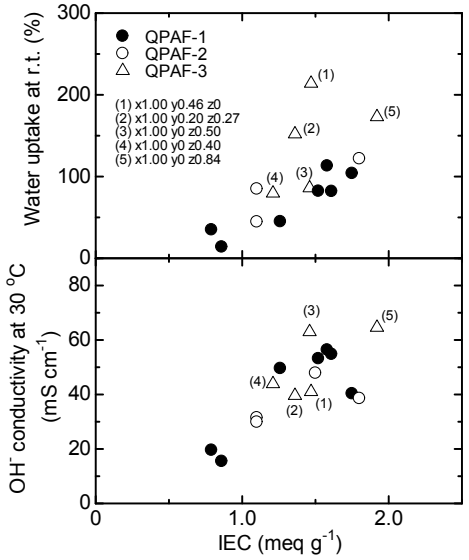

Fig. 2 Water uptake and OH^- conductivity (in water) of QPAF membranes as a function of IEC.[40,41,43]

Fig. 2 shows water uptake and hydroxide ion conductivity of the QPAF membranes in water as a function of IEC.[40,41,43] Data with various *m*- / *p*-phenylene ratios in the hydrophilic moieties (y/z ratios) of QPAF-3 are included. In most cases, the water uptake increased with increasing IEC values and/or the *m*-phenylene content in the hydrophilic moieties of QPAF-3. Compared with QPAF-1 and -2 membranes, QPAF-3 membranes showed higher water uptake, suggesting that the introduction of flexible alkylene groups into the hydrophilic moieties of the main chain might cause more swelling and thus higher water uptake for the QPAF-3 membranes.

The hydroxide ion conductivity of the QPAF membranes increased with increasing IEC values when the IEC was lower than ca. 1.5 meq g^{-1}. At higher IEC, the conductivity of QPAF-1 and -2 membranes dropped and that of QPAF-3 membrane showed a plateau, probably because high water uptake and swelling caused the lower carrier ion concentration. It is noticeable that the ion conductivity increased with increasing *p*-phenylene content of QPAF-3 membrane, i.e., the opposite dependence from that of the water uptake. Fig. 3 shows the temperature dependence of the hydroxide ion conductivities of the selected QPAF membranes in water.[40,41,43] All membranes exhibited Arrhenius-type temperature dependence of the ion conductivity from 30 to 80 °C. The apparent activation energy for the hydroxide ion conduction of the QPAF membranes was estimated from the slope to be 11.7 kJ mol^{-1} for QPAF-1 (IEC = 1.26 meq g^{-1}), 12.6 kJ mol^{-1} for QPAF-2 (1.0 meq g^{-1}), and 11.9 kJ mol^{-1} for QPAF-3 (1.46 meq g^{-1}), which were similar to the reported values for AEMs and 1 M KOH aqueous solution (9.4 kJ mol^{-1}).[33,36] This result indicates that they share a similar ion-conducting mechanism involving hydrated OH^- ions, as in alkaline aqueous solution. Among these membranes, QPAF-3 membrane (IEC = 1.46 meq g^{-1}) achieved the highest conductivity of 123 mS cm^{-1} at 80 °C.

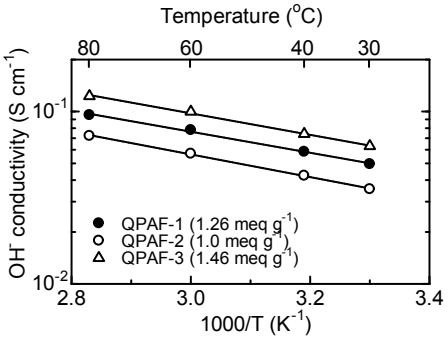

Fig. 3 Temperature dependence of OH^- conductivity (in water) of QPAF membranes.[40,41,43]

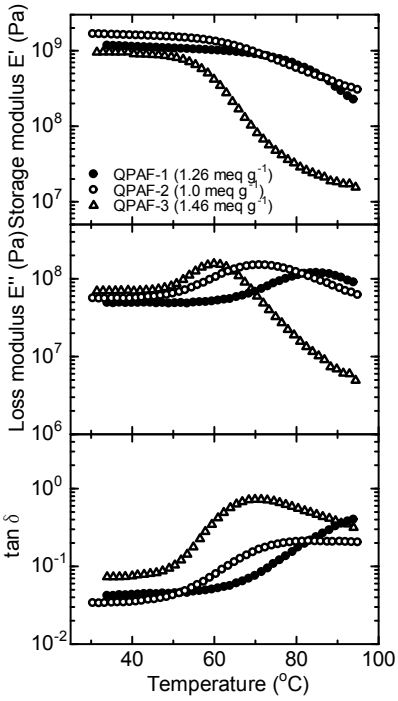

Fig. 4 DMA analyses of QPAF-1 (51 μm), QPAF-2 (53 μm), and QPAF-3 (70 μm) membranes (in Cl^- forms) at 60% RH as a function of temperature.[40,41,43]

Fig. 4 shows temperature dependence of the storage moduli (E'), loss moduli (E''), and tan δ (= E''/E') of the QPAF membranes at 60% RH.[40,41,43] The E' values of all of the QPAF membranes decreased with increasing temperature. In addition, all of the QPAF membranes exhibited broad peaks in E'', which might be associated with a glass transition. The observed T_g values were in the order QPAF-1 (ca. 85 °C) > QPAF-2 (ca. 70 °C) > QPAF-3 (ca. 60 °C). Taking much higher T_g for all aromatic-type AEMs (i.e., without perfluoroalkylene and/or alkylene groups in the main chain) into account, the

effect on pushing up T_g was in the order phenylene > perfluoroalkylene > alkylene groups in the main chain.

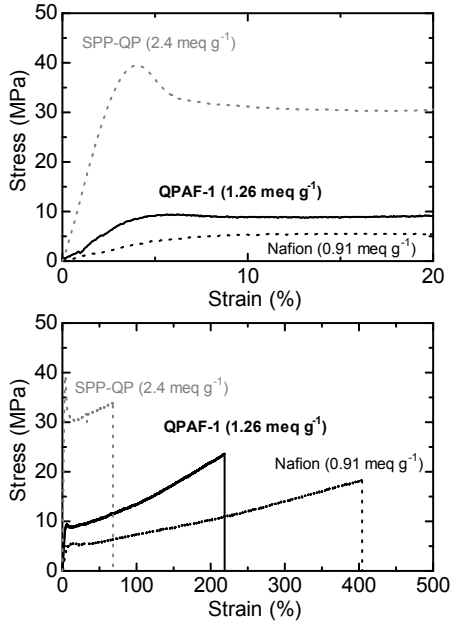

Fig. 5 Stress versus strain curves of QPAF-1 (in Cl^- form, 53 μm) membrane at 80 °C and 60% RH.[40] For comparison, data of Nafion (as a perfluorinated membrane, 50 μm) and SPP-QP[51] (as a perfluoro-group-free polyphenylene-type membrane, 84 μm) are also included. Both membranes were in H^+ forms. Note that Nafion and SPP-QP are PEMs (proton conductors), while QPAF-1 is an AEM.

Fig. 5 shows stress-strain curve of the QPAF-1 membrane as a representative QPAF at 80 °C and 60% RH.[40] For comparison, data for Nafion (as a pure perfluorinated-type) and SPP-QP[51] (as a pure, perfluoro-group-free polyphenylene-type) membranes are also included, while the ionic groups were different (sulfonic acid groups). Note that Nafion and SPP-QP are PEMs (proton conductors), while QPAF-1 is an AEM. Since the main chain of QPAF-1 consists solely of perfluoroalkylene and phenylene groups, the mechanical properties of QPAF-1 were located between those of the Nafion and SPP-QP membranes, i.e., Young's modulus and yield stress were in the order SPP-QP > QPAF-1 > Nafion, and elongation was in the order Nafion > QPAF-1 > SPP-QP. This result indicates that the presence of perfluoroalkylene groups in the main chain decreases Young's modulus and yield stress and increases elongation, whereas the phenylene groups in the main chain function in the reverse way. Although further consideration should be included, since the molecular structure of the ionic groups and the crystallinity or morphological aspects might affect the mechanical properties, we could see some aspects of the hybrid molecular nature in the QPAF-1 membrane.

Another interesting feature was observed in gas permeation properties of the membranes (Fig. 6), which strongly affects the performance and durability of fuel cells. Specifically, hydrogen and oxygen gas crossover decreases cell voltage and causes risk of device failure. It is well known that aromatic-type ionomer membranes have smaller gas permeability than that of perfluorinated-type ionomer membranes, which is in good accordance with the lower gas permeability of SPP-QP than that of Nafion membranes (Fig. 6). Interestingly, the gas permeability of QPAF-1 did not lie between those of Nafion and SPP-QP membranes but was closer to that of SPP-QP. It is recognized that, in thin ionomer membranes, the hydrophobic domains offer a major pathway for the gases. The partially aromatized main chain structure may be responsible for the much lower gas permeability of QPAF-1 than that of Nafion. The estimation of gas diffusivity and solubility as well as detailed morphological analysis will help clarify the details of this result. In any case, QPAF-1 membranes possessed good gas barrier properties, which are advantageous for practical fuel cell applications.

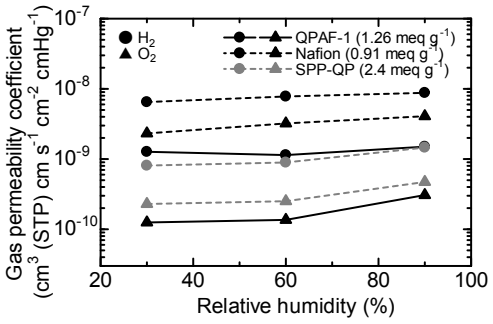

Fig. 6 Hydrogen and oxygen permeability of QPAF-1 (in Cl^- form) membrane at 80 °C as a function of RH.[40] For comparison, data of Nafion (as a perfluorinated membrane) and SPP-QP[51] (as a perfluoro-group-free polyphenylene-type membrane) are also included. Both membranes were in H^+ form. Note that Nafion and SPP-QP are PEMs (proton conductors), while QPAF-1 is an AEM.

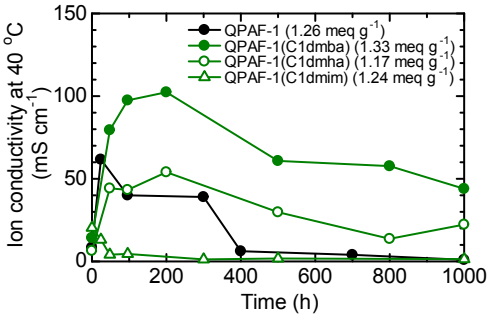

Fig. 7 Alkaline stability of the QPAF-1[40] and QPAF-1(C1R)[44] (discussed in the following section) membranes in 1 M KOH at 60 °C. The ion conductivity at 40 °C in water is plotted as a function of testing time. Note that data in this figure include the progress of the ion exchange reaction; i.e., the increase in conductivity during the initial several tens of hours is related to the ion exchange reaction from the Cl^- form to the OH^- form.

Alkaline stability of the QPAF membranes was tested in 1 M KOH aqueous solution at 60 °C, and the ion conductivity at 40 °C was monitored as a function of testing time up to 1000 h. (Note that the absolute alkaline stability of AEMs might depend not just on the OH^- concentration and time, but also on the hydration level.[18]) As a representative, data for QPAF-1 membrane (IEC = 1.26 meq g^{-1}, Cl^- form) are shown in Fig. 7.[40] In the initial 24 h, the conductivity jumped from 8.4 mS cm^{-1} to 61.7 mS cm^{-1} due to the ion exchange reaction from the Cl^- form to the more conductive OH^- form. The conductivity decreased gradually with testing time down to 1.0 mS cm^{-1} (1.6% retention) after 1000 h. The post-test QPAF-1 membrane retained its shape and bendability, however, lost its solubility in organic solvents, indicative of some structural changes including the polymer main chain such as cross-linking. The IR spectrum (data not shown) of the post-test membrane did not show evidence of degradation in the perfluoroalkylene groups, but suggested some degradation in the ammonium groups, which accounted for the decrease in the conductivity during the alkaline stability test. The QPAF-3 membrane sharing the same ammonium group (i.e., benzyltrimethylammonium groups) showed similar alkaline instability,[43] suggesting the need for replacement of the benzyltrimethylammonium groups with other ammonium groups for improving the stability.

QPAFs with other ammonium groups on benzyl scaffold (QPAF-1(C1R)[44])

Recently, several researchers claimed that introduction of pendant alkyl groups at the benzylic nitrogen-centered cation enhanced the alkaline stability and/or conductivity. An example is the comb-shaped poly(phenylene oxide) (PPO), which typically possesses one long alkyl chain at the benzylic nitrogen-centered cation.[20,52,53] It was reported that QC6-PPO, a comb-shaped PPO having pendant hexyl groups, showed better stability compared with QPPO, a non-comb-shaped PPO, i.e., QC6-PPO-40 (IEC_{tit} = 2.13 meq g^{-1}) maintained 56.5% of its initial conductivity after 720 h in 1 M NaOH at 80 °C, which was higher than that (38.8%) for QPPO-40 (IEC_{tit} = 2.27 meq g^{-1}). To investigate the effect of the pendant aliphatic ammonium groups on our QPAF-1 membrane, we selected C4 (dimethylbutylammonium; dmba) and C6 (dimethylhexylammonium; dmha) as the pendant alkyl chain length (Fig. 8). The investigation was further extended to heterocyclic ammonium groups (dimethylimidazolium; dmim).[44] Note that these QPAF-1(C1R)s were synthesized from the chloromethylated precursor (CMPAF), as shown in Scheme 1a.

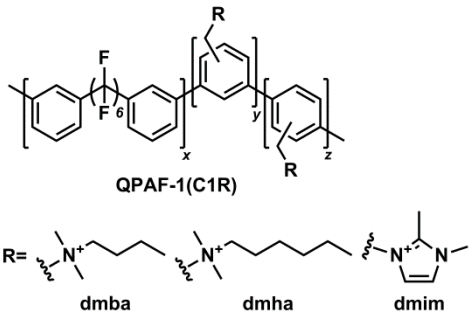

Fig. 8 Chemical structure of QPAF-1(C1R)[44].

Synthesis of QPAF-1(C1R)[44]

The synthetic procedure was almost the same with the aforementioned QPAF-1 (Scheme 1), except for the quaternization reaction. Specifically, the quaternization reaction was conducted with amine (dimethylbutylamine for dmba, dimethylhexylamine for dmha, and 1,2-dimethylimidazole for dmim) in methanol at 60 °C for 48 h (in a homogeneous system) since these amines are not soluble in water. The recovered QPAF-1(C1R) solid was cast from NMP solution to obtain QPAF-1(C1R) membrane (in Cl^- form), which was a procedure similar to that for QPAF-1. By changing the copolymer composition and the degree of quaternization (DQ), QPAF-1(C1R) with titrated IEC ranging from 0.49 to 1.33 meq g^{-1} were successfully synthesized.[44]

Properties of QPAF-1(C1R)[44]

The effect of the ammonium groups on water uptake at room temperature in water was investigated for the membranes in OH^- forms (Fig. 9).[40,44] QPAF membranes with pendant aliphatic groups exhibited comparable water uptake: 45%, 43%, and 45% for QPAF-1 (C1dmha) (IEC = 1.17 meq g^{-1}), QPAF-1 (C1dmba) (IEC = 1.16 meq g^{-1}), and QPAF-1 (IEC = 1.26 meq g^{-1}), respectively. This result suggested negligible or minor dependence of the water uptake on aliphatic side chains attached with the ammonium groups. On the other hand, QPAF-1 (C1dmim) (IEC = 1.24 meq g^{-1}) with comparable IEC exhibited much larger water uptake (120%) than the others, probably because of the strong hydrophilicity of the imidazolium rings. Regarding hydroxide ion conductivity of QPAF membranes in water at 30 °C, QPAF-1 (C1dmba) (IEC = 1.33 meq g^{-1}) achieved the highest conductivity (87 mS cm^{-1}) for its relatively low water uptake, which was one of the highest hydroxide ion conductivities for QPAF membranes in water at 30 °C. Similar to the QPAF-1, -2, and -3 membranes in Fig. 3, selected QPAF-1(C1R) membranes also showed Arrhenius-type temperature dependence of the conductivity in the temperature range of 30-80 °C (data not shown).[44] The apparent activation energies were 13.3 kJ mol^{-1} for QPAF-1(C1dmha) (IEC = 1.17 meq g^{-1}), 10.0 kJ mol^{-1} for QPAF-1(C1dmba) (IEC = 1.33 meq g^{-1}), and 9.2 kJ mol^{-1} for QPAF-1(C1dmim) (IEC = 1.24 meq g^{-1}), which were similar to those of the aforementioned QPAF membranes, such as 11.7 kJ mol^{-1}

for QPAF-1 (IEC = 1.26 meq g^{-1}). This result indicated that the effect of these ammonium groups on the ion-conducting mechanism was minor. On the other hand, the maximum conductivity at 80 °C was in the order 152 mS cm^{-1} for QPAF-1 (C1dmba) (IEC = 1.33 meq g^{-1}) > 101 mS cm^{-1} for QPAF-1 C1dmha) (IEC = 1.17 meq g^{-1}) > 96 mS cm^{-1} for QPAF-1 (IEC = 1.26 meq g^{-1}) > 65 mS cm^{-1} for QPAF-1(C1dmim) (IEC = 1.24 meq g^{-1}).

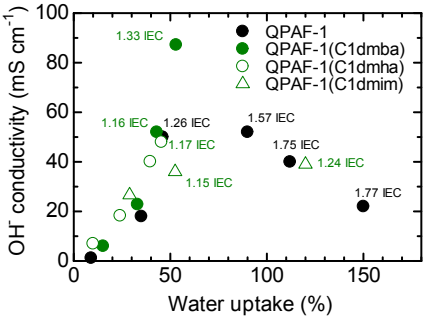

Fig. 9 OH^- conductivity (in water) of QPAF-1[40] and QPAF-1(C1R)[44] membranes at 30 °C as a function of water uptake.

To understand the reason for the enhanced conductivity of the QPAF-1(C1dmba) and QPAF-1(C1dmha) membranes, the morphology of the selected QPAF-1(C1R) membranes was observed by TEM images (data not shown).[44] Similar to the aforementioned QPAF-1 (C1 as pendant alkyl groups), QPAF-1(C1R) membranes also showed small phase-separated morphologies. The hydrophilic domain size was in the order ca. 2-8 nm for QPAF-1(C1dmha) (IEC = 1.17 meq g^{-1}) > ca. 2-6 nm for QPAF-1(C1dmba) (IEC = 1.33 meq g^{-1}) > ca. 1-2 nm for QPAF-1(C1dmim) (IEC = 1.24 meq g^{-1}) ≈ ca. 1-2 nm for QPAF-1 (IEC = 1.26 meq g^{-1}) in diameter. This result indicates that the introduction of pendant alkyl groups (C4 or C6, in this case) at the benzylic nitrogen-centered cation might promote self-aggregation of the ammonium groups, which might have contributed to the aforementioned enhanced ion conductivity in QPAF-1(C1dmba) and QPAF-1(C1dmha) membranes. In the SAXS profiles (Fig. 10), however, no clear difference was observed between QPAF-1(C1dmba) (IEC = 1.33 meq g^{-1}, in Cl^- form) and QPAF-1 (IEC = 1.26 meq g^{-1}, in Cl^- form) membranes, probably because of the insufficient periodicity of the morphology. Regarding the QPAF-1(C1dmim) membrane, the observed smaller domain size might result from the compact and planar imidazolium rings.[54] The smaller domain size (observed in TEM image under dry conditions, data not shown) as well as much larger water uptake (Fig. 9) is accountable for the lower conductivity of the QPAF-1(C1dmim) membrane.[44] In this case, the latter might be the main reason because the excess water in QPAF-1(C1dmim) membrane caused swelling, resulting in the lower carrier concentration compared to that of QPAF-1 membrane with similar IEC. Further morphological studies are needed to clarify the location and the role of excess water.

Fig. 7 includes alkaline stability of QPAF-1(C1R) membranes in 1 M KOH at 60 °C.[44] As mentioned above, the conductivity of the QPAF-1 (C1 as pendant alkyl groups) membrane decreased significantly under these conditions. After 1000 h, the remaining conductivity (at 40 °C) and the retention of conductivity were 43.95 mS cm^{-1} and 56% for QPAF-1(C1dmba), 22.3 mS cm^{-1} and 50% for QPAF-1(C1dmha), 1.4 mS cm^{-1} and 6.87% for QPAF-1(C1dmim), and 1.0 mS cm^{-1} and 1.6% for QPAF-1. Thus, taking both the remaining conductivity and the retention of conductivity into account, the alkaline stability was in the order QPAF-1(C1dmba) > QPAF-1(C1dmha) > QPAF-1(C1dmim) ≈ QPAF-1. The higher alkaline stability of the ammonium groups with pendant alkyl groups would be because of the steric shielding effect, i.e., the flexible alkyl chains around the benzylic nitrogen-centered cation were likely to mitigate the attack by hydroxide ions, which is in accordance with previous studies.[20,52,53] However, it was reported that the benzyl group was likely to facilitate the decomposition of quaternary ammonium groups in alkaline media, because the benzyl group could enhance the electrophilicity of quaternary ammonium groups and could stabilize the benzylic radical or anion intermediates among the degradation pathways.[55] Thus, the removal of the benzyl ammonium groups seemed to be the crucial next step to further enhance the alkaline stability of our QPAF membranes, in particular, under much severer conditions.

Sustainable Energy & Fuels

PERSPECTIVE

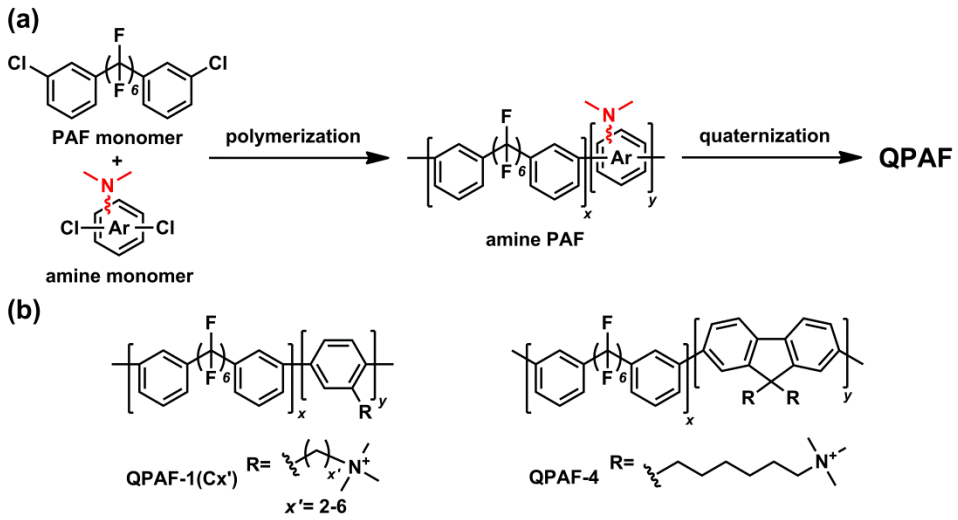

Scheme 2 (a) Synthesis and (b) molecular structure of QPAF-1(Cx')[45] and -4[46] via preaminated monomer route.

QPAFs with pendant ammonium head groups (QPAF-1(Cx')[45] and QPAF-4[46])

The benzyl ammonium groups are vulnerable to the alkaline environment even when β hydrogen atoms are not present. Some researchers independently claimed that the introduction of interstitial aliphatic groups between the main chain and ammonium group enhanced the alkaline stability, mitigating some degradation reactions such as nucleophilic substitution (S_N2) and Hofmann (β hydrogen atoms) elimination. For example, TMAC6PP, Diels-Alder poly(phenylene), with trimethylammonium groups attached by a hexamethylene spacer, exhibited improved alkaline stability in 4 M KOH at 90 °C.[25] After 336 h, the retention of conductivity was ca. 95% without loss in IEC, which was much higher than those (ca. 67% retention of conductivity, 79% retention of IEC) for ATMPP (a benzyltrimethylammonium counterpart). We speculated that a similar effect could be expected in our QPAF membranes.

For this purpose, we investigated two series of QPAF membranes (Scheme 2). (i) QPAF-1(Cx')[45]: The main chain consisted of PAF and phenylene. (ii) QPAF-4[46]: The main chain consisted of PAF and fluorene. In both cases, trimethylammonium groups were attached through interstitial alkyl (C2-6 for i and C6 for ii) groups. The results were compared systematically to determine the optimum molecular structure for AEMs.

Synthesis of QPAF-1(Cx')[45] and QPAF-4[46]

For both cases, the synthetic procedure involved preaminated monomer (Scheme 2a). It consisted of preaminated monomer synthesis, Ni-mediated copolymerization, and quaternization, followed by ion exchange reactions. This route enabled us to precisely control the position of the ammonium groups, as well as to diversify the chemical structure of the ammonium groups, which was difficult or impossible with the aforementioned chloromethylation route (Scheme 1a).

The copolymerization of the PAF monomer and the corresponding dimethylaminated monomer was carried out under similar conditions to Scheme 1a, to provide high molecular weight polymers. Note that, in Scheme 2, neutralization (e.g., with K_2CO_3 aq) of the protonated dimethylamine groups in the amine PAFs should be carefully conducted before the following quaternization reaction with methylation agents.[45,46]

For QPAF-1(Cx'), the quaternization reaction took place with dimethyl sulfate in DMAc at room temperature for 48 h. The recovered QPAF-1(Cx') solid was cast from NMP solution to obtain QPAF-1(Cx') membranes in methylsulfate ion forms, which was a similar procedure to that described above for QPAF-1 and QPAF-1(C1R) membranes. For QPAF-4, the quaternization reaction was carried out with iodomethane in DMAc at room temperature for 24 h, followed by direct casting to obtain QPAF-4 membranes in I^- forms. In any case, the counter-anions (i.e., $CH_3SO_4^-$ or I^-) were suitably converted to OH^-, Cl^-, and $PtCl_4^{2-}$, depending on the measurements. By changing the copolymer composition, QPAF-1(Cx') (IEC_{tit} = 0.92-1.65 meq g^{-1}) and QPAF-4 (IEC_{tit} = 0.75-1.84 meq g^{-1}) were

attainable. The solubility of those QPAFs was high; i.e., QPAF-1(Cx') was soluble in some polar organic solvents such as ethanol, NMP, DMSO and DMAc, and QPAF-4 was also soluble in DMSO, DMAc, methanol (with IEC higher than 1.47 meq g^{-1}), and acetone (with IEC lower than 1.02 meq g^{-1}). The high solubility, in particular in low boiling-point solvents such as methanol or ethanol, is beneficial for its use as an electrolyte binder in fuel cell catalyst layers.

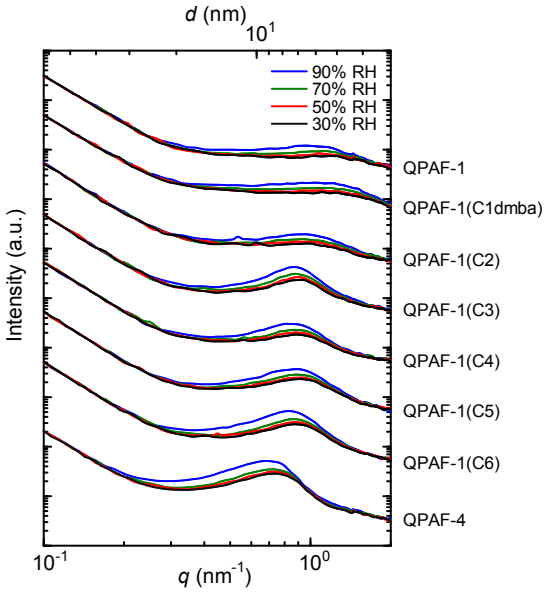

Fig. 10 SAXS profiles (in Cl^- forms) of QPAF membranes as a function of the scattering vector (q) value at 40 °C.[40,44,45,46]

Properties of QPAF-1(Cx')[45] and QPAF-4[46]

QPAF-4 membrane (in $PtCl_4^{2-}$ forms) exhibited a similar, well-developed phase-separated morphology to that of QPAF-1 membrane (in $PtCl_4^{2-}$ form), confirmed by TEM measurement (data not shown).[46] The hydrophilic and hydrophobic domains of QPAF-4 were spherical, ca. 1.5 nm in diameter, which was similar to that of QPAF-1 (both domains were ca. 1-2 nm in diameter, as shown in Fig. 1a), despite the large difference in molecular structure. On the other hand, SAXS profiles strongly depended on the molecular structure, in particular, the interstitial chain length between the main chain and the ammonium group (Fig. 10).[40,44,45,46] As the interstitial chain length increased, the ionomer peak became prominent and the *d* spacing became larger. The comparison between QPAF-1(C1dmba) and QPAF-1(C4) suggested that the ammonium groups located at the terminal of the side chains developed more phase separation. Furthermore, comparison between QPAF-1(C6) and QPAF-4 suggested that not only the polymer main chain but also the position or density of the ammonium group-tethered side chains affected the morphology. The larger size of the ionomer peak in QPAF-4 than QPAF-1(C6) suggested that the dense ammonium groups contributed more to the phase separation. Among the QPAF membranes, QPAF-4 exhibited the largest ionomer peak, much larger than that of the QPAF-1 membrane. The difference in the results from the TEM images and SAXS profiles was probably due to the different counter-ions and measurement conditions (in particular, humidity).

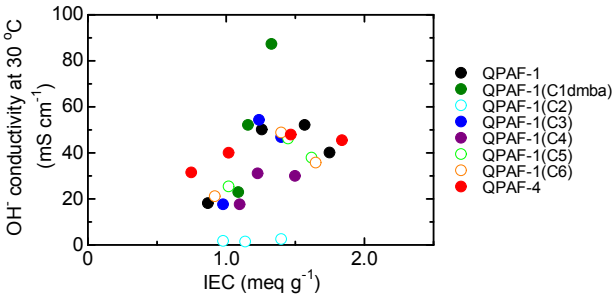

Fig. 11 Hydroxide ion conductivity of QPAF membranes at 30 °C in water as a function of IEC.[40,44,45,46]

Fig. 11 shows the hydroxide ion conductivity of the membranes at 30 °C in water as a function of IEC.[40,44,45,46] All QPAF-1(Cx') and QPAF-4 membranes exhibited a similar behavior with QPAF-1, i.e., a volcano type dependence of the hydroxide ion conductivity on the IEC. An exception was QPAF-1(C2), whose hydroxide ion conductivity was very low, because of its low water absorbability (e.g., the water uptake of QPAF-1(C2, 0.98 meq g^{-1}) and (C3, 0.98 meq g^{-1}) were 7.24% and 48.56% at 60 °C).[45] Much less developed ion channels of QPAF-1(C2) might be responsible, although the reason of such low water absorbability is unclear. Further studies (e.g., introduction of the C2 groups in other polymer systems) might help understand this unusual property.

All QPAF-1(Cx') and QPAF-4 membranes showed an approximate Arrhenius-type temperature dependence of the conductivity (data not shown).[45,46] The apparent activation energy (E_a) was 10.5 kJ mol^{-1} for QPAF-1(C3) (IEC = 1.24 meq g^{-1}), 6.5 kJ mol^{-1} for QPAF-1(C4) (IEC = 1.23 meq g^{-1}), 6.8 kJ mol^{-1} for QPAF-1(C5) (IEC = 1.45 meq g^{-1}), 11.0 kJ mol^{-1} for QPAF-1(C6) (IEC = 1.40 meq g^{-1}), and 9.8-11.3 kJ mol^{-1} for QPAF-4 (IEC = 0.75 - 1.84 meq g^{-1}), similar to that of the aforementioned QPAF membranes having the benzyl ammonium groups. This result indicated that the introduction of the interstitial aliphatic group between the main chain and ammonium group did not affect the ion conduction mechanism. An exception was the QPAF-1(C2) membrane (IEC = 1.14 meq g^{-1}), whose E_a (19.6 kJ mol^{-1}) was much higher than those of the other membranes due to its much smaller water uptake and thus much less developed ion channels, even under the wet conditions. The maximum hydroxide ion conductivity at 80 °C in water was in the order QPAF-1(C1dmba) (1.33 meq g^{-1}) (152 mS cm^{-1}) >> QPAF-1(C3) (1.24 meq g^{-1}) (99 mS cm^{-1}) ≈ QPAF-1 (1.26 meq g^{-1}) (98 mS cm^{-1}) > QPAF-1(C6) (1.40 meq g^{-1}) (93 mS cm^{-1}) > QPAF-4 (1.47 meq g^{-1}) (86.2 mS cm^{-1}) > QPAF-1(C5) (1.45 meq g^{-1}) (69 mS cm^{-1}) > QPAF-1(C4) (1.23 meq g^{-1}) (64 mS cm^{-1}) >> QPAF-1(C2) (1.5 meq g^{-1}) (4 mS cm^{-1}).

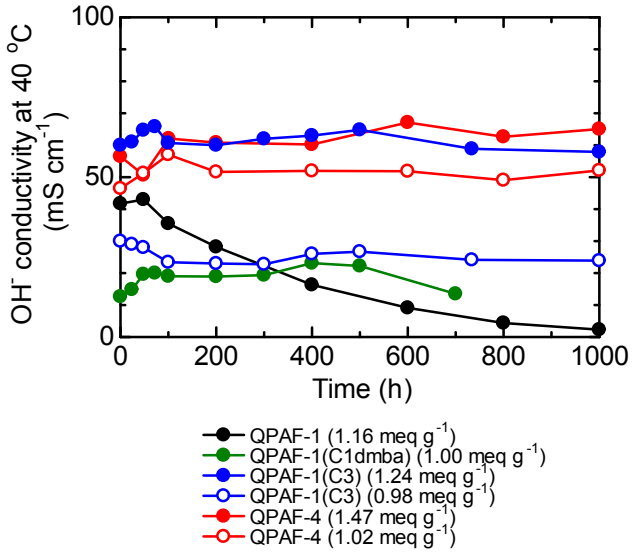

Fig. 12 Alkaline stability of QPAF membranes in 1 M KOH at 80 °C.[40,44,45,46] The conductivity at 40 °C in water is plotted as a function of testing time. Note that data in this figure do not include the process of ion exchange reaction.

The alkaline stability of QPAF membranes was tested in 1 M KOH at 80 °C (Fig. 12),[40,44,45,46] higher temperature than in Fig. 7 (60 °C). Since (i) QPAF-1(C4), -1(C5), and -1(C6) membranes absorbed much water and became gels above 60 °C and (ii) the conductivity of the QPAF-1(C2) membrane was too low, only the results of QPAF-1(C3) were included for the QPAF-1(Cx') membranes. The QPAF-1 membrane, having benzyltrimethylammonium groups, showed a gradual decrease in hydroxide ion conductivity from 43.0 mS cm^{-1} (data after 48 h, as the initial conductivity) to 2.3 mS cm^{-1} after 1000 h, which corresponded to the small retention of conductivity (ca. 5%). The QPAF-1(C1dmba) membrane, containing benzyldimethylbutylammonium groups, showed improved alkaline stability, and the remaining conductivity and the retention of conductivity after 700 h were 13.5 mS cm^{-1} and 68% (calculated based on the data after 48 h, as the initial conductivity), respectively. After the test, both QPAF-1 and QPAF-1(C1dmba) membranes became insoluble in organic solvents, which made it difficult to investigate structural analyses such as solution NMR.[40,44] Significant enhancement in alkaline stability was observed for QPAF-1(C3) and QPAF-4 membranes, both of which possessed an interstitial aliphatic group between the main chain and ammonium group.[45,46] The QPAF-1(C3) membrane exhibited high remaining conductivity and high retention of conductivity after 1000 h; 57.9 mS cm^{-1} and 98% for a membrane with IEC = 1.24 meq g^{-1}, and 24 mS cm^{-1} and 80% for a membrane with IEC = 0.98 meq g^{-1}, respectively. The highest stability was observed for QPAF-4 membranes, i.e., the remaining conductivity and the retention of conductivity after 1000 h were 65.1 mS cm^{-1} and ~100% for a membrane with IEC = 1.47 meq g^{-1}, and 52.1 mS cm^{-1} and ~100% for a membrane with IEC = 1.02 meq g^{-1}. QPAF-1(C3) and QPAF-4 membranes retained solubility in organic solvents, which qualitatively indicated minor structural degradation. In the case of QPAF-1(C3) membrane (IEC = 0.98 meq g^{-1}), the retention of IEC was 90% (titration) and 73% (^{1}H NMR), respectively. In the case of QPAF-4 membrane (IEC = 1.47 meq g^{-1}), no practical changes in the molecular structure (^{1}H and ^{19}F NMR) and the mechanical properties (S-S curves) were confirmed, verifying its stability in 1 M KOH at 80 °C for 1000 h.

Alkaline stability and durability of various AEMs

Table 1 summarizes the alkaline stability of various AEMs including our QPAFs. In the "Other AEMs" category, some alkaline stable AEMs (at least, in 1 M NaOH (or KOH) at 80 °C for long periods of time) recently reported in the literature from various institutes were selected. In most cases, the AEMs do not contain (i) aromatic-ether linkages in the main chain and (ii) benzyltrimethylammonium groups, because these groups are vulnerable in such harsh alkaline environments. One exception here is NC5Q-PPO, which is a poly(2,6-dimethyl-1,4-phenylene oxide) (PPO) with an interstitial aliphatic group between the main chain and alkyltrimethylammonium group.[20] The NC5Q-PPO membrane retained the IEC (≥ 83%) and conductivity (≥ 80%) in 1 M NaOH at 80 °C for 720 h. Under similar conditions, C4-AEM [a poly(ethylene-co-tetrafluoroethylene) (ETFE)-based radiation-grafted AEM with an interstitial butyl group between the benzene and methylpyrrolidinium group],[21] PFBFF$^+$ [a poly(fluorene) with an interstitial hexyl group between the main chain and alkyltrimethylammonium group],[22] and PBPA$^+$ [a poly(biphenyl alkylene) with an interstitial aliphatic group between the main chain and alkyltrimethylammonium group][23] were also durable. In particular, PBPA$^+$ seemed the most prominen,t because the post-test PBPA$^+$ exhibited the highest hydroxide ion conductivity (124 mS cm^{-1} in water at 80 °C) with nearly perfect retention of the conductivity and IEC, even after testing in 1 M NaOH at 80 °C for 720 h.

Some AEMs have been claimed to be durable under even harsher conditions. PTPipQ1, a poly(arylene piperidinium) without aryl ether bonds or benzylic sites, retained IEC (≈95%) in 2 M NaOH at 90 °C for 360 h.[24] TMAC6PP, a Diels-Alder poly(phenylene) with an interstitial hexyl group between the main chain and alkyltrimethylammonium group, maintained IEC (~100%) and conductivity (95%) in 4 M KOH at 90 °C for 336 h.[25]

PMP-TMA-41, a polyolefin-based AEM with a bulky side chain and an interstitial aliphatic C9 chain between the main chain and alkyltrimethylammonium group, retained IEC (> 90%) and conductivity (> 92%) in 10 M NaOH at 80 °C for 700 h.[26] HMT-PMPI, a poly(arylene imidazolium) sterically protected around the C2-position, retained IEC (> 95%) in 10 M KOH at 100 °C for 168 h.[27]

More recently, Dekel et al. reported that the number of water molecules solvating the hydroxide ion strongly affected the stability of the quaternary ammonium groups.[56,57] The nucleophilicity and basicity of the hydroxide ion increased with decreasing hydration number of the hydroxide ion, resulting in the rapid degradation of the quaternary ammonium groups. In

operating fuel cells, the cathode binder and/or membrane at high current density would experience ultra-low hydration levels, resulting in much faster degradation in the fuel cell than in the ex-situ alkaline stability test in concentrated alkaline aqueous solution.

To evaluate the durability (and performance) in practical operating fuel cells, a hydrazine alkaline fuel cell using QPAF-4 as the membrane and electrolyte binder was operated at 60 °C with 1 M KOH containing 10 wt% hydrazine as a fuel and humidified oxygen or air as an oxidant.[46] Note that fuel cell testing in our laboratory was conducted under practical conditions: low platinum loading, no back-pressure, and practical flow rate (typically, 100 mL min^{-1}) and fuel/oxygen utilization (i.e., avoiding operating with extremely low utilizations). Consequently, the fuel cell achieved high maximum power densities of 515 mW cm^{-2} at a current density of 928 mA cm^{-2} with oxygen and 323 mW cm^{-2} at a current density of 696 mA cm^{-2} with air. The durability was also evaluated in an operating fuel cell at a constant current density of 20 mA cm^{-2} at 60 °C. Although the cell voltage gradually decreased from 0.77 V to 0.51 V after 1067 h, the recovered QPAF-4 membrane did not show any mechanical failure, with no detectable pinholes, proving that the QPAF-4 membrane functioned well, with reasonable durability in an operating fuel cell.[46] Although further detailed post-test analyses need to be conducted, the voltage loss may suggest a lack of durability when less than adequately hydrated or when in contact with catalysts.

In addition, an H_2/O_2 fuel cell using QPAF-1(C3) as the membrane and electrolyte binder was also operable at 60 °C and 100% RH for both O_2 and H_2.[45] The maximum power density of the QPAF-1(C3) cell was 224 mW cm^{-2}, ca. 1.8 times higher than that of the Tokuyama A201 (a benchmark AEM) cell (122 mW cm^{-2}) and even higher than those of our previous QPAF-1(C1dmba) (167 mW cm^{-2}) and QPAF-1 (138 mW cm^{-2}) cells. The durability was evaluated in an operating fuel cell at a constant current density of 50 mA cm^{-2} at 60 °C and 100% RH. After 62 h operation, the QPAF-1(C3) cell maintained 69% of its initial voltage which was also superior to that of the Tokuyama A201 cell (52% remaining voltage). Post-test NMR analyses implied that the voltage loss in the QPAF-1(C3) cell seemed to be attributed more to the electrolyte binder degradation and/or morphological changes but not structural degradation, which was not contradictory to the aforementioned reports of Dekel et al.[56,57] In fact, the alkaline stability of the QPAF-1(C3) membrane decreased with increasing concentration of alkaline solution (Table 1), and the conductivity significantly decreased in 8 M KOH at 80 °C for 568 h (remaining conductivity of 4-9 mS cm^{-1}, retention of conductivity of 9-14%).[45]

The high durability of QPAF-4 and QPAF-1(C3) membranes in the operating fuel cells suggested that the introduction of the interstitial aliphatic side chains led to significant enhancement, not only in the ex-situ alkaline stability of the membranes but also in the operating fuel cell performance and durability.[45,46] For practical AEMFC applications, however, development of more durable AEMs under harsher alkaline conditions, such as higher concentration of alkaline solution or the presence of hydroxide ion with ultra-low hydration level at higher temperature, will be essential. Further, development of AEMFCs which are durable with much higher current densities and prolonged operation time will also be needed.

Sustainable Energy & Fuels

PERSPECTIVE

Table 1 Alkaline stability of various AEMs

Sample	Initial properties			Test condition			Post-test properties				Ref.
	IEC (meq g^{-1})		Conductivity (mS cm^{-1})	Alkali	Temperature (°C)	Time (h)	Retention (%)			Conductivity (mS cm^{-1})	
							IEC		Conductivity		
	Titration	NMR					Titration	NMR			
QPAFs											
QPAF-1	-	1.16	95.5 (OH^-, 80 °C, in water)	1M KOH	80	1000	-	-	5	2.3 (OH^-, 40 °C, in water)	40
QPAF-3	1.46	1.56	122.8 (OH^-, 80 °C, in water)	1M KOH	80	1000	-	-	< 1	0.1 (OH^-, 40 °C, in water)	43
QPAF-1(C1dmba)	1.00	1.15	22.8 (OH^-, 30 °C, in water)	1M KOH	80	700	-	-	68	13.5 (OH^-, 40 °C, in water)	44
QPAF-1(C3)	0.98	1.04	17.5 (OH^-, 30 °C, in water)	1M KOH	80	1000	90	73	80	24 (OH^-, 40 °C, in water)	45
				4 M KOH	80	1000	85	96	74	24 (OH^-, 40 °C, in water)	
				8 M KOH	80	568	-	93	9	4 (OH^-, 40 °C, in water)	
	1.24	1.51	99 (OH^-, 80 °C, in water)	1M KOH	80	1000	-	-	98	57.9 (OH^-, 40 °C, in water)	
				4 M KOH	80	1000	77	96	73	43 (OH^-, 40 °C, in water)	
				8 M KOH	80	568	71	92	14	9 (OH^-, 40 °C, in water)	
QPAF-4	1.02	1.13	71.8 (OH^-, 80 °C, in water)	1M KOH	80	1000	-	-	≈100	52.1 (OH^-, 40 °C, in water)	46
	1.47	1.62	86.2 (OH^-, 80 °C, in water)	1M KOH	80	1000	-	≈100	≈100	65.1 (OH^-, 40 °C, in water)	
Other AEMs[a]											
NC5Q-PPO-40	2.03	-	73.9(OH^-, 80 °C, in water)	1 M NaOH	80	720	91	-	90	66.4 (OH^-, 80 °C, in water)	20

NC5Q-PPO-60	2.57	-	96.1(OH^-, 80 °C, in water)	1 M NaOH	80	720	83	-	80	76.9 (OH^-, 80 °C, in water)	
C4-AEM	1.51	-	30.4 (Cl^-, 60 °C, in water)	1 M KOH	80	672	87	-	-	-	21
$PFBFF^+$	2.93	2.89	85 (OH^-, 80 °C, in water)	1 M NaOH	80	720	99	91	-	-	22
$PBPA^+$	2.70	2.61	122 (OH^-, 80 °C, in water)	1 M NaOH	80	720	98	≈100	≈100	124 (OH^-, 80 °C, in water)	23
PTPipQ1	2.42	-	89 (OH^-, 80 °C, in water)	2 M NaOH	90	360	-	≈95	-	-	24
TMAC6PP	1.74	2.20	17.4 (Cl^-, r.t., in water)	4 M KOH	90	336	≈100	-	95	16.6 (Cl^-, r.t., in water)	25
PMP-TMA-41	1.92	-	75.2 (OH^-, 80 °C, in water)	10 M NaOH	80	700	>90	-	>92	-	26
HMT-PMPI	-	2.61	10 (Cl^-, 25 °C, in water)	10 M KOH	100	168	-	>95	-	-	27

[a] NC5Q-PPO: a poly(2,6-dimethyl-1,4-phenylene oxide) (PPO) with interstitial aliphatic group between main chain and alkyltrimethylammonium group. C4-AEM: a poly(ethylene-co-tetrafluoroethylene) (ETFE)-based radiation-grafted AEM with interstitial butyl group between benzene and methylpyrrolidinium group. $PFBFF^+$: a poly(fluorene) with interstitial hexyl group between main chain and alkyltrimethylammonium group. $PBPA^+$: a poly(biphenyl alkylene) with interstitial aliphatic group between main chain and alkyltrimethylammonium group. PTPipQ1: a poly(arylene piperidinium) without aryl ether bonds or benzylic sites. TMAC6PP: a Diels-Alder poly(phenylene) with interstitial hexyl group between main chain and alkyltrimethylammonium group. PMP-TMA-41: a polyolefin-based AEM with bulky side chain and interstitial aliphatic C9 chain between main chain and alkyltrimethylammonium group. HMT-PMPI: a poly(arylene imidazolium) sterically protected around the C2-position.

Conclusions

We have developed a novel series of QPAFs as AEMs for alkaline fuel cell applications. First, we have examined the effect of the perfluoroalkylene groups in the polymer main chains on the AEM properties, and found that QPAFs exhibited superior AEM properties, including well-developed phase-separated morphology, good hydroxide ion conductivity, mechanical robustness, and gas barrier properties. Furthermore, QPAFs survived in a harsh alkaline environment because of the polymer main chains made up of C-C bonds only; however, the benzyltrimethylammonium groups on the QPAFs degraded significantly. Then, we have examined the effect of the molecular structures of the quaternary ammonium groups on the alkaline stability of QPAF membranes and found that the quaternary ammonium groups having the interstitial aliphatic groups between the main chains and ammonium groups were clearly more stable. The comparison of our QPAFs with other state-of-the-art AEMs has revealed that our QPAFs are some of the most alkaline-durable and highly anion-conductive AEMs.

The results discussed herein indicate that the well-designed aromatic, partially fluorinated AEMs are potentially applicable to AFCs that use hydrogen or hydrazine as a fuel. However, there still remain some issues to be addressed. These include the development of more alkaline-durable cationic head groups under harsher conditions (e.g., higher concentration of alkaline solution or the presence of hydroxide ion with ultra-low hydration level, at higher temperature). This will lead to

better performing cathode electrolyte binders and/or membranes, enabling long-term operation of AFCs at much higher current density. We believe that further optimization of molecular structure and morphology, and in some cases, use of reinforcement materials, will facilitate the development of high performance, robust binders, AEMs, and AEMFCs.

Conflicts of interest

There are no conflicts to declare.

Acknowledgements

This work was partly supported by Japan Science and Technology Agency (JST) through CREST (JPMJCR12C3) and by the Ministry of Education, Culture, Sports, Science and Technology (MEXT) Japan through a Grant-in-Aid for Scientific Research (18K04746, 18H02030, 18H05515, 18K19111). The authors thank Tosoh Finechem Co. for supplying 1,6-diiodo-dodecafluorohexane.

Notes and references

1 T. Sata, *J. Membr. Sci.*, 2000, **167**, 1–31.
2 J. R. Varcoe and R. C. T. Slade, *Fuel Cells*, 2005, **5**, 187–200.
3 M. A. Hickner, *Mater. Today*, 2010, **13**, 34–41.
4 J. Pan, C. Chen, L. Zhuang and J. Lu, *Acc. Chem. Res.*, 2012, **45**, 473–481.
5 M. A. Hickner, A. M. Herring and E. B. Coughlin, *J. Polym. Sci. Part B Polym. Phys.*, 2013, **51**, 1727–1735.
6 J. R. Varcoe, P. Atanassov, D. R. Dekel, A. M. Herring, M. A. Hickner, P. A. Kohl, A. R. Kucernak, W. E. Mustain, K. Nijmeijer, K. Scott, T. Xu and L. Zhuang, *Energy Environ. Sci.*, 2014, **7**, 3135–3191.
7 S. Gottesfeld, D. R. Dekel, M. Page, C. Bae, Y. Yan, P. Zelenay and Y. S. Kim, *J. Power Sources*, 2018, **375**, 170–184.
8 D. R. Dekel, *J. Power Sources*, 2018, **375**, 158–169.
9 C. G. Arges and L. Zhang, *ACS Appl. Energy Mater.*, 2018, **1**, 2991−3012.
10 E. J. Park and Y. S. Kim, *J. Mater. Chem. A*, 2018, **6**, 15456–15477.
11 K. Asazawa, K. Yamada, H. Tanaka, A. Oka, M. Taniguchi and T. Kobayashi, *Angew. Chem. Int. Ed.*, 2007, **46**, 8024–8027.
12 S. Lu, J. Pan, A. Huang, L. Zhuang and J. Lu, *Proc. Natl. Acad. Sci. U. S. A.*, 2008, **105**, 20611–20614.
13 E. S. Davydova, S. Mukerjee, F. Jaouen and D. R. Dekel, *ACS Catal.*, 2018, **8**, 6665−6690.
14 S. Chempath, J. M. Boncella, L. R. Pratt, N. Henson and B. S. Pivovar, *J. Phys. Chem. C*, 2010, **114**, 11977–11983.
15 G. Merle, M. Wessling and K. Nijmeijer, *J. Membr. Sci.*, 2011, **377**, 1–35.
16 G. Couture, A. Alaaeddine, F. Boschet and B. Ameduri, *Prog. Polym. Sci.*, 2011, **36**, 1521–1557.
17 C. E. Diesendruck and D. R. Dekel, *Curr. Opin. Electrochem.*, 2018, **9**, 173–178.
18 S. Willdorf-Cohen, A. N. Mondal, D. R. Dekel and C. E. Diesendruck, *J. Mater. Chem. A*, 2018, **6**, 22234–22239.
19 S. Pusara, S. Srebnik and D. R. Dekel, *J. Phys. Chem. C*, 2018, **122**, 11204–11213.
20 J. Pan, J. Han, L. Zhu and M. A. Hickner, *Chem. Mater.*, 2017, **29**, 5321−5330.
21 J. Ponce-Gonzalez, I. Ouachan, J. R. Varcoe and D. K. Whelligan, *J. Mater. Chem. A*, 2018, **6**, 823–827.
22 W.-H. Lee, A. D. Mohanty and C. Bae, *ACS Macro Lett.*, 2015, **4**, 453−457.
23 W.-H. Lee, Y. S. Kim and C. Bae, *ACS Macro Lett.*, 2015, **4**, 814−818.
24 J. S. Olsson, T. H. Pham and P. Jannasch, *Adv. Funct. Mater.*, 2018, **28**, 1702758.
25 M. R. Hibbs, *J. Polym. Sci. Part B Polym. Phys.*, 2013, **51**, 1736–1742.
26 M. Zhang, C. Shan, L. Liu, J. Liao, Q. Chen, M. Zhu, Y. Wang, L. An and N. Li, *ACS Appl. Mater. Interfaces*, 2016, **8**, 23321−23330.
27 J. Fan, A. G. Wright, B. Britton, T. Weissbach, T. J. G. Skalski, J. Ward, T. J. Peckham and S. Holdcroft, *ACS Macro Lett.*, 2017, **6**, 1089-1093.
28 R. C. T. Slade and J. R. Varcoe, *Solid State Ionics*, 2005, **176**, 585–597.
29 L. Wang, J. J. Brink, Y. Liu, A. M. Herring, J. Ponce-Gonzalez, D. K. Whelligan and J. R. Varcoe, *Energy Environ. Sci.*, 2017, **10**, 2154–2167.
30 A. D. Mohanty, C. Y. Ryu, Y. S. Kim and C. Bae, *Macromolecules*, 2015, **48**, 7085−7095.
31 T. H. Pham, J. S. Olsson and P. Jannasch, *J. Mater. Chem. A*, 2018, **6**, 16537–16547.
32 A. G. Wright, T. Weissbach and S. Holdcroft, *Angew. Chem. Int. Ed.*, 2016, **55**, 4818–4821.
33 K. Miyatake, B. Bae and M. Watanabe, *Polym. Chem.*, 2011, **2**, 1919–1929.
34 M. Tanaka, K. Fukasawa, E. Nishino, S. Yamaguchi, K. Yamada, H. Tanaka, B. Bae, K. Miyatake and M. Watanabe, *J. Am. Chem. Soc.*, 2011, **133**, 10646–10654.
35 J. Miyake, K. Fukasawa, M. Watanabe and K. Miyatake, *J. Polym. Sci. Part A Polym. Chem.*, 2014, **52**, 383–389.
36 J. Miyake, M. Watanabe and K. Miyatake, *Polym. J.*, 2014, **46**, 656–663.
37 N. Yokota, M. Shimada, H. Ono, R. Akiyama, E. Nishino, K. Asazawa, J. Miyake, M. Watanabe and K. Miyatake, *Macromolecules*, 2014, **47**, 8238−8246.
38 C. Fujimoto, D.-S. Kim, M. Hibbs, D. Wrobleski and Y. S. Kim, *J. Membr. Sci.*, 2012, **423–424**, 438–449.
39 C. G. Arges and V. Ramani, *Proc. Natl. Acad. Sci. U. S. A.*, 2013, **110**, 2490–2495.
40 H. Ono, J. Miyake, S. Shimada, M. Uchida and K. Miyatake, *J. Mater. Chem. A*, 2015, **3**, 21779–21788.
41 M. Ozawa, T. Kimura, R. Akiyama, J. Miyake, J. Inukai and K. Miyatake, *Bull. Chem. Soc. Jpn.*, 2017, **90**, 1088–1094.
42 M. Ozawa, T. Kimura, K. Otsuji, R. Akiyama, J. Miyake, M. Uchida, J. Inukai and K. Miyatake, *ACS Omega*, 2018, **3**, 16143−16149.
43 H. Ono, J. Miyake, K. Miyatake, *J. Polym. Sci. Part A: Polym. Chem.*, 2017, **55**, 1442–1450.
44 A. M. A. Mahmoud, A. M. M. Elsaghier, K. Otsuji and K. Miyatake, *Macromolecules*, 2017, **50**, 4256−4266.
45 A. M. A. Mahmoud and K. Miyatake, J. Mater. Chem. A, 2018, 6, 14400–14409.
46 H. Ono, T. Kimura, A. Takano, K. Asazawa, J. Miyake, J. Inukai and K. Miyatake, *J. Mater. Chem. A*, 2017, **5**, 24804–24812.
47 M. G. Marino, J. P. Melchior, A. Wohlfarth, K. D. Kreuer, *J. Membr. Sci.*, 2014, **464**, 61–71.
48 N. Ziv, W. E. Mustain, D. R. Dekel, *ChemSusChem*, 2018, **11**, 1136–1150.
49 N. Ziv, D. R. Dekel, *Electrochem. Commun.*, 2018, **88**, 109–113.
50 A. Kusoglu and A. Z. Weber, *Chem. Rev.*, 2017, **117**, 987–1104.
51 J. Miyake, R. Taki, T. Mochizuki, R. Shimizu, R. Akiyama, M. Uchida and K. Miyatake, *Sci. Adv.*, 2017, **3**, eaao0476.
52 N. Li, T. Yan, Z. Li, T. Thurn-Albrecht and W. H. Binder, *Energy Environ. Sci.*, 2012, **5**, 7888–7892.

53 N. Li, Y. Leng, M. A. Hickner and C. Y. Wang, *J. Am. Chem. Soc.*, 2013, **135**, 10124–10133.
54 A. M. A. Mahmoud, A. M. M. Elsaghier and K. Miyatake, *RSC Adv.*, 2016, **6**, 27862–27870.
55 M. G. Marino and K. D. Kreuer, *ChemSusChem*, 2015, **8**, 513–523.
56 D. R. Dekel, M. Amar, S. Willdorf, M. Kosa, S. Dhara and C. E. Diesendruck, *Chem. Mater.*, 2017, **29**, 4425–4431.
57 D. R. Dekel, S. Willdorf, U. Ash, M. Amar, S. Pusara, S. Dhara, S. Srebnik and C. E. Diesendruck, *J. Power Sources*, 2018, **375**, 351–360.

Graphical Abstract

Progress, potential and remaining challenges of state-of-the-art anion exchange membranes (AEMs), in particular, our quaternized poly(arylene perfluoroalkylene)s (QPAFs), for alkaline fuel cell applications, are overviewed and discussed.